Available online at www.sciencedirect.com
ScienceDirect
Journal of Hazardous Materials 140 (2007) 518–526
Journal of Hazardous Materials
www.elsevier.com/locate/jhazmat

The influence of ice formation on vaporization of LNG on water surfaces

V. Vesovic *

Department of Earth Science and Engineering, Imperial College London, London SW7 2BP, UK

Available online 20 October 2006

Abstract

The spillage of LNG on water surfaces can lead, under certain circumstances, to a decrease in the surface temperature of water and subsequent freezing. A model for heat transfer from water to LNG is proposed and used to calculate the surface temperature of water and examine its influence on the vaporization rate of LNG. For this purpose LNG was modeled based on the properties of pure methane. It was concluded that when LNG spills on a confined, shallow-water surface the surface temperature of water will decrease rapidly leading to ice formation. The formation of an ice layer, that will continue to grow for the duration of the spill, will have a profound effect upon the vaporization rate. The decreasing surface temperature of ice will decrease the temperature differential between LNG and ice that drives the heat transfer and will lead to a change of the boiling regime. The overall effect would be that the vaporization flux would first decrease during the film boiling; followed by an increase during the transition boiling and a steady decrease during the nucleate boiling.

Keywords: LNG; Ice formation; Vaporization rate; Modeling

1. Introduction

The demand for natural gas has been steadily increasing over the years. It is expected that by 2010 natural gas will account for a quarter of the world's primary energy consumption. This increase in demand is mainly driven by economic incentives, but the environmental concerns of using 'cleaner fuels' should not be discounted. One of the contributions to the economic incentives has been a number of technological improvements in natural gas transportation, leading to a significant cost reduction. World-wide requirements necessitate long-distance marine transportation and for economic reasons natural gas is cooled to 112 K, liquefied and transported in the liquid state. The ships carrying liquefied natural gas (LNG) are usually double-hulled and carry, on average loads of 60,000 tonnes, distributed between four and six individual tanks. As the world trade in LNG is expanding and more storage and handling facilities are being built there is an underlying concern about the consequences of an LNG accident; especially since the hazards nowadays may include intentional acts of sabotage. While the LNG industry lays claim to an exceptional safety record, regulators remain unconvinced, primarily because potential consequences of an LNG spillage can lead to a large scale accident.

In order to identify the major hazards involved it is useful to review the physical processes which take place in the spillage of LNG on water. The source of spillage can be either located above or below the water surface depending where the damage to the ship or handling facilities has occurred. In either case some of the liquid released will instantaneously flash while the rest, being much lighter than water, will spread over the surface quite rapidly. During this initial period rapid phase transition (RPT) can occur, as drops of LNG are quickly vaporized by the surrounding water, leading to the formation of a shock wave. Simultaneously with spreading on the surface of the water, the LNG will vaporize forming a vapor cloud above the pool. If there is a nearby source of ignition this will lead to a pool fire which will further enhance the vaporization process and might spread to the tanker. If the pool does not ignite immediately a vapor cloud will form. Because of its low temperature the vapor cloud formed above the pool will be denser than the surrounding air. It will travel away from the pool at the prevailing wind speed, slowly mixing with the surrounding air. Under these conditions the vapor cloud will be asphyxiating and highly flammable. If it encounters a source of ignition it can lead to either a slow burning flash fire or much less likely rapid fireball. If the vapor cloud enters a confined space then deflagration, with resulting damage caused by overpressure, may ensue.

It is thus clear from this short expose that the hazards associated with LNG spillage are varied and potentially dangerous. The modeling, for the purposes of risk assessment, of all possible

* Tel.: +44 20 7594 7352; fax: +44 20 7594 7444.
E-mail address: v.vesovic@imperial.ac.uk.

0304-3894/$ – see front matter © 2006 Elsevier B.V. All rights reserved.
doi:10.1016/j.jhazmat.2006.10.039

outcomes is difficult as it requires understanding and quantification of a number of different physical mechanisms. Although the work on elucidating different aspects of LNG spillage started in the 1970's, there are still areas that are poorly understood. A couple of recent reviews [1,2] give a good insight into our current understanding, summarizing what has been achieved and where the main areas of current interest are. In this paper we will concentrate on one of the crucial factors that determines the formation and the future behavior of the hazardous vapor cloud, namely the rate of vaporization of the LNG. In particular we are interested in modeling the rate of vaporization before the ignition occurs, during the stage where the main heat source, driving the vaporization, is the body of water over which the LNG spreads.

A number of workers have addressed this problem, both theoretically [3–8] and experimentally [9–11]. A number of field experiments have been performed over the years, where the rate of vaporization has been measured [see Ref. [2] for the summary of the field trials]. Significant advances have been made and some useful models have been proposed. Nevertheless, due to the inherent complexity of LNG vaporization on water no complete description has yet been produced. The difficulty lies in successfully describing the spreading of one liquid on top of the other taking into account a simultaneous heat transfer and subsequent bubble formation and vaporization. Even the ideal process is difficult to describe mathematically, as both the spillage rate [12] and the composition of the remaining LNG liquid [8] can vary with time. The complexity is further increased by having to consider the possibility that the boiling regime can change, that the composition gradients can develop within the LNG leading to non-equilibrium considerations, and that the temperature gradient can develop within the water leading to the possibility of ice formation. A complete description is made intractable if one tries to consider the effect of waves, currents, wind and turbulence induced by LNG on the dynamics of pool spreading and the subsequent effects on the rate of vaporization. The consequences of all these phenomena are currently not well understood.

The present project has concentrated on elucidating one particular aspect of the vaporization of LNG that has hitherto been neglected; namely, the effect of ice formation on vaporization rate. As the LNG spreads over the water surface, the water surface is exposed to a fluid at a much lower temperature. The difference in temperature of the order of 180 K is the norm. Prolonged contact will cause the water temperature to decrease. If it falls below 273 K, an ice layer will form. Further contact between LNG and the ice layer will lead to an increase in ice thickness. In a number of small scale experiments [10,11] the water surface temperature was observed to decrease rapidly with the subsequent formation of an ice layer. The presence of an ice layer not only changed the rate at which the heat was transferred to the LNG, but also led to the collapse of the film boiling, thus drastically altering the heat transfer mechanism. In spills on an unconfined water surface and in deep water, no substantial ice has been observed [3,13]. Although, in the Maplin Sands tests [2,14] there is some evidence that a thin ice layer did form [15]. The formation of ice is primarily driven by how quickly the heat can be transferred from the bulk to the top layer of water. Large bodies of water act as vast heat sources; the convection currents, together with constant mixing of the top layer, due to the action of waves and interfacial turbulence caused by LNG spreading, are the main mechanisms that maintain the supply of heat to the top layer. In general, it is assumed that lack of experimental evidence for ice formation signifies that the heat transferred to the surface is sufficient to prevent a decrease of water temperature.

The formation of ice will thus influence the dynamics and the rate of vaporization. Therefore, it seems to be essential both from a scientific and an industrial perspective to ascertain the importance of ice formation on the rate of vaporization of LNG on water.

2. Modeling and discussion

In a highly idealized case, the vaporization of LNG on water surface can be represented by the following simple model,

$$\frac{dM}{dt} = -m'' R^2 \tag{1}$$

$$\frac{dR}{dt} = \frac{\sqrt{AM}}{R} \tag{2}$$

where M and R are the mass and the radius, respectively, of the LNG pool. The parameter m'' is proportional to the vaporization rate per unit area, while parameter A characterizes the velocity of the leading edge of the LNG pool. Both parameters will be discussed, in more detail, shortly. This simple model represents the backbone of most models currently in use and although realistic in its main features, it cannot be expected to mimic the full behavior of a real spillage. Its main use, however, is in its ability to provide a simple vehicle for testing different physical mechanisms and their influence on the vaporization rate.

In order to generate this model it has been assumed that the LNG is released instantaneously, from the point source just above the water surface. The cryogen being lighter than water, would then spread on the water surface radially outwards from the point source as a cylinder of radius, R. Furthermore, it has been assumed that the interaction between the two fluids is minimal and that both surfaces can be treated as essentially flat throughout the spreading process. The spreading occurs in the gravitational-inertial regime where the height of the pool provides the driving force, while the inertia of the ambient water provides the resistance to spreading. This is a reasonable assumption, at least for spreading on unconfined water surfaces, as the high vaporization and spreading rates, lead to quick evaporation. The rate of spreading, given by Eq. (2), can be derived either by means of shallow layer theory [16,17] or 'box models' [18,19] with the parameter A given by

$$A = 2.69 \left[\frac{g(\rho_w - \rho_{LNG})}{\pi \rho_{LNG} \rho_w} \right] \tag{3}$$

where ρ_w and ρ_{LNG} are the density of water and LNG, respectively. The value of the numerical constant in Eq. (3) is usually determined experimentally, as our present knowledge of the physical conditions at the cryogen leading edge is still inade-

quate. In this work we have kept the same value as in our previous work [8] as no new experimental data have been subsequently published. It is important to stress that the derivation of Eq. (2) is based on spreading of a non-vaporizing liquid. Evaluating the constant by recourse to experimental data [17], albeit LPG data [20], can be thus seen as adjusting for vaporization, to a certain extent.

It is further assumed that the major heat source, in these type of models, is the body of water underneath. Again, this is a reasonable assumption supported primarily by estimations of heat transfer from other sources of heat [7,21,22]. Traditionally, it has been assumed that LNG boils in the film boiling regime on water. As, this is not always the case, we have not a priori chosen a mode of boiling, but have allowed for a more general behavior. The heat transfer will be driven by large temperature difference between LNG and water, with the constant of proportionality being the heat transfer coefficient h. Hence, the parameter m'' in Eq. (1) can be written as,

$$m'' = \frac{\pi h(T_w - T_{LNG})}{L_{LNG}} \tag{4}$$

where L_{LNG} is the latent heat and T_w and T_{LNG} are the temperatures of the top surface of water and of the bulk LNG, respectively. If the film boiling is indeed the mode of boiling then there will exist a thin, stable layer of vapor between water and LNG and the h will refer to the heat transfer coefficient of the LNG vapor film. If the vaporization occurs in the transitional regime, then the film will be unstable, partially collapsing and regenerating itself and h will represent some average heat transfer coefficient. We allow for the formation of a thin thermal layer in water, from the water surface downwards, where the temperature will not correspond to the bulk temperature. Fig. 1 illustrates the schematic of the described heat transfer mechanism.

In order to calculate the rate of vaporization of LNG one needs to solve the coupled first-order differential equations, Eqs. (1) and (2). This can be easily achieved providing all the quantities entering the description of parameters A and m'' are known. This is not as straightforward, as it would seem. There are a number of issues that increase the complexity of the model, that primarily arise from the compositional nature of LNG and the cooling of the top water layer.

LNG is a mixture of hydrocarbons, dominated by methane. Although methane is usually present, by volume, in quantities of the order of 85–95%, the boiling of LNG is both qualitatively and quantitatively different to that of pure methane. As LNG vaporizes, the more volatile component (methane) will vaporize preferentially and the remaining liquid LNG will get richer in the heavier components (ethane, propane, . . .). This will result in the boiling point of the remaining liquid increasing as a function of time. The latent heat of the remaining liquid will also vary, usually increasing, but in some cases, at the later stages of the spill, a decrease is observed [8]. Hence the model presented in Eqs. (1)–(4) has to be supplemented by the thermodynamic phase equilibria calculation that will allow for the variation of T_{LNG} and L_{LNG} with composition and consequently as a function of spill duration. Such simulations have been performed [8] and they show that the vaporization rate in the final stages of the spill is markedly different to that of pure methane, leading to longer spill times. Furthermore, the simulations indicated that at the later stages of the spill, as the aged LNG becomes ethane rich, the film boiling is replaced by transition boiling leading to higher vaporization rates.

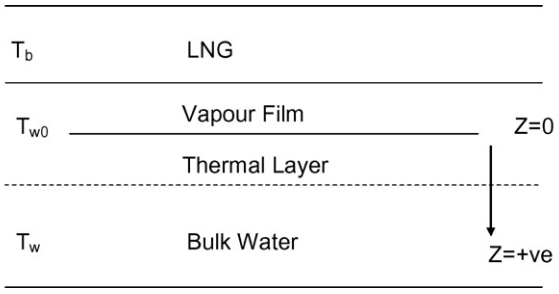

Fig. 1. Schematic of vaporization of LNG on a liquid water surface.

Initial stages of LNG boiling exhibit certain peculiarities. It has been observed in a number of experiments [10,11] that the initial rate of vaporization of LNG exceeds that of pure methane. No quantitative model has been proposed, so far, that could adequately describe this phenomena, although a number of possible scenarios have been suggested. It has been proposed [10,23] that the amount of heat being transferred to LNG leads to the bottom layer of LNG, nearest to the heating surface, to rapidly become depleted in methane and hence not have enough time to re-establish equilibrium with the bulk LNG. As a consequence the boiling temperature of the fluid contained in this layer will increase which will result in a decrease of vapor production. This in turn will lead to a collapse of the film and the change of the boiling regime. A change away from the film boiling mode will lead to much higher heat fluxes which in turn will produce the observed increase in vaporization rate.

Hence, we can see that the changes in composition of the thin layer of LNG can lead to the change in the mode of boiling; thus, requiring supplementing the described model by reliable predictions of the heat transfer coefficient as a function of the spill duration. The prediction of heat transfer coefficient for LNG or for any mixture in general is difficult due to a lack of experimental data and reliable correlations. This is especially true for the transition boiling regime.

Finally, the temperature of water over which LNG is spilling can also be affected, as discussed in the Introduction; especially if the body of water is either confined or shallow, or the amount of surface mixing is small, there will be insufficient heat arriving at the surface to keep it at constant temperature. Under such circumstances the model, given by Eqs. (1)–(4) has to be supplemented by a model that can predict the onset of ice formation and a model that can estimate the heat transfer coefficient in the presence of ice layer.

Thus, a simple model presented above needs a number of auxiliary models before one can use it to predict the vaporization rate of LNG. It would be thus useful to develop a reference model which has a minimal number of auxiliary models to be used as the benchmark case for comparison. Fortunately, treating LNG as composed of pure methane, which is equivalent to ignoring compositional effects, provides us with such a model.

In the rest of the paper we will refer to this model as a spill of pure liquid methane, to indicate that the LNG compositional effects are being ignored. In this case the boiling temperature, together with all the thermodynamic properties entering Eqs. (3) and (4) remain constant during the duration of the spill. It is well documented that the boiling occurs in the film boiling regime and the heat transfer coefficient can be either estimated or obtained from the experimental data [8,24,25]. Thus all the quantities entering Eqs. (3) and (4), bar the water surface temperature can be taken as constant. The water surface temperature, as briefly discussed above, will depend on the mass of the body of water over which the spill occurs and on how efficient the mixing of the top layer is, due to the action of waves and interfacial turbulence. In this work we will examine two limiting scenarios. First, liquid methane spill on open water sufficiently deep and with good mixing of the top layer that we can assume that the water surface temperature remains constant through out the duration of the spill. Second, liquid methane spill over the body of water where the heat arrives to the water surface by conduction, only. A good example of this would be spills over small confined bodies of water, where the surface is essentially calm.

2.1. Limiting case—deep, unconfined water

Here we assume that T_W is constant which for the case of pure methane makes both parameters A and m'' constant throughout the duration of the spill. This greatly simplifies the basic model and gives us the ideal, reference case to which we can compare models that allow for more complex behavior. Most of the early models and quite a few of the current ones estimate the vaporization rate of the LNG by means of this reference model.

In principal, the two coupled first order differential equations, Eqs. (1) and (2) can be easily solved numerically to give the variation of both the radius and the mass of LNG pool with time. It is nevertheless instructive to also look at some analytical solutions. Combining the two first-order differential equations we can obtain the second-order differential equation,

$$\frac{d^2M}{dt^2} = -2m''A^{0.5}\sqrt{M} \equiv -B\sqrt{M}. \tag{5}$$

Eq. (5) can be integrated to give the relationship for the vaporization rate in terms of the mass remaining, namely

$$\frac{dM}{dt} = \frac{2}{\sqrt{3}}\sqrt{B}[M_0^{3/2} - M^{3/2}]^{1/2}, \tag{6}$$

where M_0 is the initial mass spilled. This expression can be further integrated, by making a substitution $x = (M/M_0)^{1/2}$, to obtain the total time of evaporation, t_f

$$t_f = \sqrt{\frac{3}{2}}\left[\frac{M_0}{(m'')^2A}\right]^{1/4}\int_0^1 \frac{x\,dx}{\sqrt{(1-x^3)}}, \tag{7}$$

$$t_f = 1.0562\left[\frac{M_0}{(m'')^2A}\right]^{1/4} \tag{8}$$

Hence, we find that the maximum evaporation time, for pure liquid methane spreading and boiling on the water surface of the constant temperature, is proportional to the fourth root of the initial mass spilled. This gives us, a very easy to use, estimate of evaporation times for liquid methane and to a certain extent for LNG as well. As a way of example, 50 tonnes ($\sim$120 m^3), of liquid methane will take approximately 2 min to completely evaporate, while 120,000 tonnes ($\sim$28,500 m^3), which is approximately the size of one individual tank on the average tanker, will take approximately 7–8 min. Hence, the process of evaporation of liquid methane on unconfined water surfaces is rapid.

The expression derived above, Eq. (8), is analogous to the one obtained recently by Fay [12] for the instantaneous spill. Furthermore, Raj and Kalelkar [26] and later Opschoor [4] derived a similar expression,

$$t_f = 0.9634\left[\frac{M_0}{(m'')^2A}\right]^{1/4}, \tag{9}$$

different to Eq. (8) only in a constant of proportionality, starting from the spreading law of the type

$$\frac{d^2R}{dt^2} = -\frac{AM}{R^3}. \tag{10}$$

Their expression, as already noted by Fay [12], gives evaporation times 10% lower than the ones calculated by means of Eq. (8). The discrepancy can be attributed to the use of two different spreading models. Both spreading models, Eqs. (2) and (10) have been derived from the considerations of non-volatile liquids. It can be actually shown by a simple differentiation of Eq. (2) that they are equivalent. Once, the models are applied to a vaporizing liquid, the equivalence breaks down. In this case, differentiating Eq. (2) produces an extra term due to variation of mass with time. It is not yet clear, without further theoretical or experimental work, what is a more accurate spreading model for LNG. Both spreading models were applied to vaporizing liquids in an ad-hoc fashion, based on the assumption that they would be valid, as long as the vaporization rate is smaller than the spreading rate. The only advantage that Eq. (2) has over Eq. (10) is that it reproduced the experimental data on spreading of vaporizing liquid, albeit LPG data.

In the case of a liquid methane spill on confined surfaces, the rate of evaporation, once the spreading has stopped, is simply given by Eq. (1). In this case the radius R is the radius of the enclosure. Assuming that the enclosure is sufficiently small, one can neglect the time it takes for liquid methane to spread and estimate the time for complete evaporation, by integrating Eq. (1). The resulting time for the complete evaporation is now proportional to the initial mass of the liquid methane spilled. This will result in a much longer vaporization times, than those calculated above, for the equivalent mass spilled. The exact values will depend on the radius of the enclosure. For instance, 50 tonnes of methane spilled in an enclosure of radius of 10 m will now take 48 min to completely evaporate. The size of enclosure is critical, since the same amount spilled will completely evaporate before the radius has grown to approximately 50 m. In real spills it is unlikely that the confined water surface will be able to maintain its surface temperature constant for such a long

duration of time. Hence, we need to examine how the presence of a spill will change the surface temperature of the water.

2.2. Limiting case—heat transfer through water by conduction only

Here we examine a different limiting case and assume that the heat transfer through a body of water is by conduction only. The temperature of the surface of the water in contact with LNG modeled as liquid methane, see Fig. 1, is now determined by the amount of heat conducted to the water surface. We assume that the predominant mode of heat transfer is in z-direction, thus making the problem one-dimensional. This is certainly true if the thermal boundary layer in water is small, compared with the radius of the methane pool. Later on, we shall show that this is indeed the case. The heat transfer through the body of water can be described by means of the Fourier conduction equation,

$$\frac{\partial T_w}{\partial t} = \kappa_w \frac{\partial^2 T_w}{\partial z^2}, \tag{11}$$

where κ_w is the thermal diffusivity of water. We assume that the water is initially, before the spillage, at some uniform temperature T_0, that the body of water is semi-infinite and that the heat removed from the surface of water is proportional to the temperature difference between the water surface and the methane pool. The initial and boundary conditions can then be written down as follows:

$$t = 0, \quad T_w = T_0,$$

$$z = \infty, \quad T_w = T_0, \tag{12}$$

$$z = 0, \quad \left.\frac{\partial T_w}{\partial z}\right|_{z=0} = \frac{h}{\lambda_w}(T_{w0} - T_b),$$

where λ_w is the thermal conductivity of water, T_{w0} the temperature of the water surface ($z=0$) and T_b is the boiling temperature of methane. Here, we have defined the positive z-direction to be downwards, opposite to the movement of heat. The Fourier conduction equation, Eq. (11), can be transformed into a standard heat conduction equation for semi-infinite media [27] by transformation $\theta = T_w - T_b$. The resulting equation has a known analytical solution [27]. The variation of the water surface temperature with time is then given by,

$$T_{w0} = T_b + (T_0 - T_b)\exp(t^*)\mathrm{erfc}(\sqrt{t^*}), \tag{13}$$

where the reduced time, t^* is given by

$$t^* = \frac{h^2}{\lambda_w^2}\kappa_w t. \tag{14}$$

A similar solution has been proposed by Waite et al. [6], but they have assumed that heat is removed by conduction through a thin vapor film. As is shown by the above derivation there is no need to assume the detailed mechanism of heat removal; especially as the proposed solution [6] then requires the knowledge of film thickness which is difficult to estimate.

When the temperature of water drops to 0 °C the top surface will start freezing and ice formation will occur. This will fundamentally change the vaporization process as will be discussed in the next section. By solving Eq. (13) for $T_{w0} = 0$ we can estimate the time it takes for ice to form. In order to perform this calculation we have assumed that liquid methane boils on the liquid water surface in the film boiling regime. Both the experimental evidence and the theoretical calculations based on Leidenfrost temperature for methane support this assumption [8–11]. The heat transfer coefficient is taken to be 155 $W\,m^{-2}\,K^{-1}$ based on theoretical calculations reported previously [8]. The value is in general agreement with experimental observations [4,10–11] of vaporization mass flux. Fig. 2 illustrates the change in surface temperature of water as a function of time, based on solution of Eq. (13). It takes approximately between 1 and 2 s for water to start freezing. The exact value is a function of the initial water temperature, as illustrated in Fig. 2. Nevertheless, irrespective of the initial water temperature and the exact value of the heat transfer coefficient, one can conclude that the drop in temperature is rapid and the ice will start forming nearly instantaneously. This is in general agreement with what has been observed experimentally [10,11].

By examining the full analytical solution of Eq. (11) one can calculate the thickness of the thermal layer in water that has been created due to presence of methane pool. The thickness calculated is of the order of a millimeter and indicates that the assumption of treating the heat conduction as a one-dimensional problem is justified. Furthermore, the model can be used in a more exploratory way to take into account some convective motion by replacing the molecular thermal conductivity with an effective parameter. A simple calculation indicates that in order to maintain the surface temperature of water to within 10 °C of the original temperature, for the spills that last up to 5 min in duration, the effective thermal conductivity has to be approximately three orders of magnitude larger than the molecular one. This gives some indication of the amount of thermal inertia that water layer provides if the conduction is the dominant mode of heat transfer.

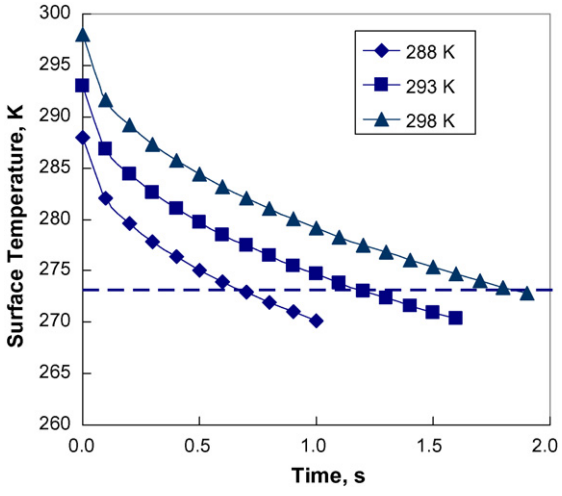

Fig. 2. Profile of the surface temperature of water following an LNG spill, as a function of three initial water temperatures.

2.2.1. Ice formation

Once the temperature of the top surface of water decreases to 0 °C the ice will start forming. The heat removed will now cause freezing of the water surface and will be provided by the latent heat of fusion of the water. Only once the top surface has frozen will the heat removed lead to further decrease of the top surface temperature. Hence, the heat transfer from the bulk of water to the methane pool above will be by conduction, first through a thermal layer of water, and then through the growing ice layer. At the point of contact between the ice layer and water extra heat will be generated by freezing of water. The schematic in Fig. 3 illustrates the new scenario. It has been assumed that the ice layer will float on water which is consistent with our assumption of ignoring the edge effects and treating the heat conduction problem in one dimension only. The heat transfer process can be modeled as follows:

$$\frac{\partial T_w}{\partial t} = \kappa_w \frac{\partial^2 T_w}{\partial z^2}, \quad z > \varepsilon \tag{15}$$

$$\frac{\partial T_i}{\partial t} = \kappa_i \frac{\partial^2 T_i}{\partial z^2}, \quad 0 \le z < \varepsilon \tag{16}$$

$$\rho_w L_w \frac{\partial \varepsilon}{\partial t} = \lambda_i \left.\frac{\partial T_i}{\partial z}\right|_{z=\varepsilon} - \lambda_w \left.\frac{\partial T_w}{\partial z}\right|_{z=\varepsilon}, \quad z = \varepsilon \tag{17}$$

where κ_i and λ_i are the thermal diffusivity and thermal conductivity, respectively of the ice layer, and ρ_w and L_w are the density at 0 °C and the latent heat of fusion, respectively of water. The following initial and boundary conditions were imposed,

$$t = 0, \quad T_w = T_{\text{initial}}(z, t),$$

$$z = \varepsilon, \quad T_w = T_f, \qquad z = \infty, \quad T_w = T_0, \tag{18}$$

$$z = 0, \quad \left.\frac{\partial T_i}{\partial z}\right|_{z=0} = \frac{h}{\lambda_i}(T_{i0} - T_b),$$

where T_{initial} is the temperature profile obtained from the analytical solution of Eq. (11), once the surface of water reaches 0 °C. That time is taken as $t = 0$ for the implementation of the ice model described above. T_f is the freezing temperature of water.

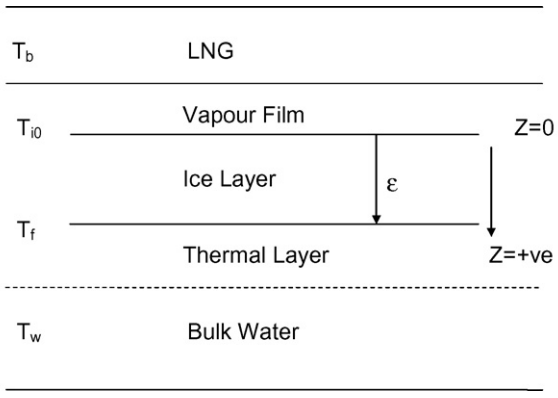

Fig. 3. Schematic of vaporization of LNG on water in the presence of ice.

The coupled differential equations, Eqs. (15)–(18) were solved by a finite-difference method proposed by Murray and Landis [28] for heat conduction problems involving freezing, that allows for a growth of the solid phase. For LNG this method was originally implemented by Valencia-Chavez and Reid [10] and most recently by Guerra [29]. The method presented here differs from the previous work in a choice of boundary conditions at the ice-methane interface. Most workers [6,9], followed the suggestion of Valencia-Chavez and Reid [10], and assumed a simple linear temperature profile for this interface based on fitting to the experimental heat flux values of the original work [10]. Here, we take a different approach and calculate the temperature profile by maintaining the heat flux across the interface, as given by Eq. (18). Hence, keeping the method fully predictive without recourse to any experimental information.

In order to implement the method, the ice region ($z < \varepsilon$) is divided into r equally spaced increments, while the water region ($z > \varepsilon$) is divided into ($N - r$) increments, where N is the total number of nodes. The top node is placed on the surface of the ice, the middle node is placed at the ice-water boundary, with the Nth node placed sufficiently deep within the water region so that the boundary condition at $z = \infty$ can be maintained. The effectiveness of this particular numerical approach [28] is that as the ice layer grows, the nodes move, increasing the size of increments in the ice layer and decreasing the ones in water. For further details of the numerical method the reader is referred to Refs. [28,29].

Although the thermal conductivity of ice is about three times that of liquid water and extra heat is being liberated by fusion of water, the heat arriving, by conduction, to the top ice surface is not sufficient to maintain it at a constant temperature. Fig. 4 illustrates the time dependence of the surface temperature of the ice. Initially, the temperature rapidly decreases, dropping to about 240 K within a few seconds. By this time the ice thickness has grown to approximately 0.5 mm. The temperature gradient across the ice layer is now sufficient to maintain a higher heat flux across the ice layer and hence the decrease of the surface

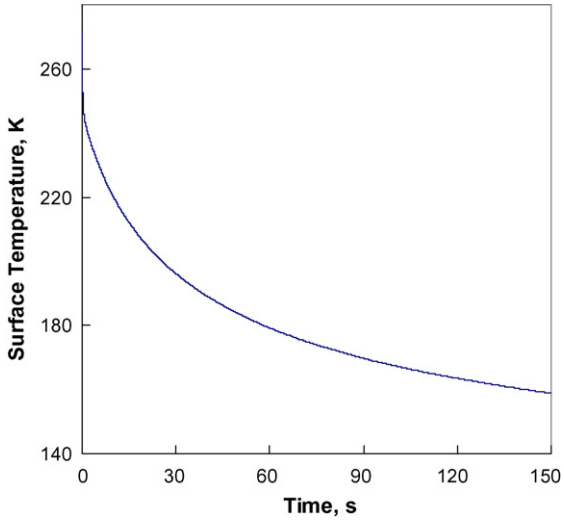

Fig. 4. Profile of the surface temperature of ice following an LNG spill.

temperature becomes less rapid. The decrease in the surface temperature, decreases the temperature differential across the vapor film and thus reduces the heat flux into the liquid methane pool. Preliminary simulations show that if the temperature profile shown in Fig. 4 is used together with a constant value of the heat transfer coefficient the vaporization times will decrease substantially. For instance, it will take approximately 40% longer to vaporize 50 tonnes of methane, than if the water temperature is maintained constant [8].

The decrease in the surface temperature of ice also influences the stability of the vapor film. As the rate of vaporization decreases, less bubbles are formed which leads to instability of the film. At some stage the minimum surface temperature or the minimum heat flux to maintain stable film boiling will be breached and the transition boiling will occur. During the transition boiling the film will be partially collapsing and regenerating itself which would lead to an increase in the average heat transfer coefficient. This would lead to a more rapid decrease in the surface temperature of ice, than can be observed in Fig. 4; but more importantly to the increase in the vaporization rate.

Preliminary simulations have been performed where the model given by Eqs. (15)–(18) was used to simulate transition boiling. The heat transfer coefficient was estimated by means of the correlation given in Ref. [25] and implemented in Ref. [8]. Simulations show that the overall effect of transition boiling would be to increase the vaporization rate, which is in agreement with the experimental observation [10]. The duration of the transition boiling is of the order of tens of seconds. It is thought prudent not to give quantitative results at this stage, due to a large uncertainty in the value of heat transfer coefficient during the transition boiling. Work is now in progress to get a better estimate of the heat transfer coefficient by recourse to experimental data.

There are a number of estimates in the literature of when the stable film boiling will no longer be sustainable. The Leidenfrost temperature of methane, which is relatively low, would indicate the collapse of film boiling at around 160 K. This assumes that the boiling occurs on the ideal surfaces that possess the infinite thermal diffusivity which would maintain the boiling surface at a constant temperature. On the surfaces with the physical properties of ice the estimates of the collapse of film boiling are when the surface temperature of ice falls below 225 K and 210 K [30,31]. Fig. 4 illustrates that this would happen within 10–15 s after the ice has been formed. So, from this point onwards we would expect the increase in the vaporization rate. The preliminary simulations indicate that the increase is observed until the value of heat flux reaches the critical value for nucleate boiling. At this point the film has completely collapsed over the whole surface and nucleate boiling is taking place.

Once the nucleate boiling regime is established, the surface temperature of ice will fall immediately to 112 K, the boiling temperature of methane. The heat transferred to methane will be by conduction only through the growing ice layer. Fig. 5 illustrates the rate at which the ice layer will grow once the nucleate boiling has occurred. Only the growth following the onset of nucleate boiling is shown. The thickness of ice increases

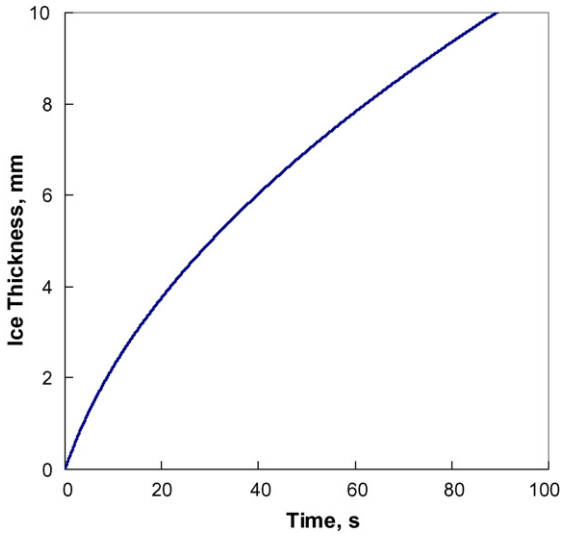

Fig. 5. Profile of the thickness of the ice layer following the onset of nucleate boiling.

nearly linearly with time and the growth rate is estimated to be $0.1\,\mathrm{mm\,s^{-1}}$.

For nucleate boiling Eq. (4) is still valid and can be used to estimate the vaporization rate with the obvious constraint that we have modeled LNG as liquid methane. The heat transfer coefficient h used in Eq. (4) now refers to ice layer and is given by

$$h = \frac{\lambda_i}{\varepsilon} \tag{19}$$

Its value decreases in time as the ice layer thickness grows, thus reducing the vaporization rate of methane. Hence, in nucleate boiling the vaporization rate is governed by the thermal properties of the ice layer.

3. Conclusions

The rate of vaporization of LNG on water depends not only on the chemical composition of LNG and the dynamics of the water surface over which the spill occurs, but also on the surface temperature of water. More importantly the change of surface temperature of water, as a consequence of the presence of the spill, will critically influence the rate of vaporization. In order to ascertain the influence of changing surface temperature on the dynamics of the vaporization we have modeled LNG as pure methane spill over an ideal, flat water surface. In this case the vaporization rate is only influenced by the time behavior of the surface temperature of water.

If the LNG spill, modeled as the liquid methane spill, occurs over unconfined, deep water, where the convection currents and the interfacial turbulence are sufficient to maintain the surface temperature of water constant, the liquid methane will vaporize at a constant flux rate, in the film boiling regime. The time for a liquid methane spill to completely evaporate on an unconfined water surface, is proportional to the fourth root of the initial mass spilled. This relationship can be used to estimate the time for the equivalent fully compositional LNG spill to evaporate.

We have also highlighted that the calculation of the time for complete evaporation is influenced by the choice of the spreading model. The spreading models based on specifying the velocity of the leading edge and the models that are based on the force balance over an element of liquid, lead to identical results when applied to spreading of non-evaporating liquids. When the models are used to simulate the spreading of evaporating liquids the difference in the calculated evaporation times is of the order of 10% as shown in Section 2.1.

In spills on confined water surfaces the presence of LNG or liquid methane will lead to a rapid decrease of the surface water temperature. The water will start freezing with an ice layer forming on the top. The formation of ice critically influences the rate of vaporization. First, the formation of ice will lead to a further decrease in surface temperature, thus decreasing the temperature difference between the liquid methane and the heating surface, which will result in a continuous decrease of the vaporization rate as a function of spill duration. Secondly, the drop in the temperature difference will lead to a collapse of the vapor film and change of the boiling regime; initially to a transition and then to nucleate boiling. It is estimated that the transition boiling will start within 10–15 s after the ice has formed or after the spill has been initiated. This type of boiling will lead to the increase in the vaporization rate. Once the nucleate boiling starts the surface temperature of ice will drop to the boiling temperature of methane. The vaporization rate will now be governed by the amount of heat conducted through the growing ice layer and will decrease with time.

In the boiling of liquid methane on water surface we distinguish two regimes. Initially the thermal inertia of the thin vapor film governs the amount of heat transferred to liquid methane, while later on the thermal inertia of a growing ice layer takes over.

It is important to emphasise that we have here considered two limiting cases, which give us a valuable insight into the LNG spreading and vaporization, but we do not purport to claim that the models presented will account for the full complexity of a real LNG spill.

Simulations are currently being carried out to compare the vaporization rates of pure methane to a scant experimental data [10,11]. Further simulations are being planned to elucidate the vaporization rate of LNG on confined water surfaces, by means of the models described above, in order to test how the composition of LNG will influence the conclusions reached for methane.

Acknowledgements

The author would like to thank his former MSc student, Mr. Enrique Guerra, for initial developments of the computer code for heat conduction in the presence of growing solid phase.

References

[1] M. Hightower, L. Gritzo, A. Luketa-Hanlin, J. Covan, S. Tieszen, G. Wellman, M. Irwin, M. Kaneshige, B. Melof, C. Morrow, D. Ragland, Guidance on risk analysis and safety implications of a large liquefied natural gas (LNG) spill over water, Sandia Report, SAND2004-6258, December 2004.

[2] A. Luketa-Hanlin, A review of large-scale LNG spills: experiments and modeling, J. Hazard. Mater. 132 (2006) 119–140.

[3] B. Otterman, Analysis of large LNG spills on water, Cryogenics (1975) 455–460, and references therein.

[4] G. Opschoor, Investigation into spreading and evaporation of LNG spilled on water, Cryogenics (1977) 629–633.

[5] P. Shaw, F. Briscoe, Vaporization of spills of hazardous liquids on land and water, UKAEA Report SRD R100, 1978.

[6] P.J. Waite, R.J. Whitehouse, E.B. Winn, W.A. Wakeham, The spread and vaporization of cryogenic liquids on water, J. Hazard. Mater. 8 (1983) 165–184.

[7] D.M. Webber, A model for pool spreading and vaporization and its implementation in the computer code GASP, UKAEA Report SRD R507, 1990.

[8] C. Conardo, V. Vesovic, The influence of chemical composition on vaporization of LNG and LPG on unconfined water surfaces, Chem. Eng. Sci. 55 (2000) 4549–4562.

[9] E.M. Drake, A.A. Jeje, R.C. Reid, Transient boiling of liquefied cryogens on a water surface, Int. J. Heat Mass Transfer 18 (1975) 1361–1368; E.M. Drake, A.A. Jeje, R.C. Reid, Transient boiling of liquefied cryogens on a water surface, Int. J. Heat Mass Transfer 18 (1975) 1369–1375.

[10] J.A. Valencia-Chavez, R.C. Reid, The effect of composition on the boiling rates of liquefied natural gas for confined spills on water, Int. J. Heat Mass Transfer 22 (1979) 831–838.

[11] R. Boe, Pool boiling of hydrocarbon mixtures on water, Int. J. Heat Mass Transfer 41 (1998) 1003–1011.

[12] J.A. Fay, Model of spills and fires from LNG and oil tankers, J. Hazard. Mater. B96 (2003) 171–188.

[13] G.F. Feldbauer, Spills of LNG on water. Esso Research and Engineering Report, EE61E-72, 1972.

[14] J.S. Puttock, D.R. Blackmore, G.W. Colenbrander, Field experiments on dense gas dispersion, J. Hazard. Mater. 6 (1982) 13–41, and references therein.

[15] Shell Global Solutions, Private Communication.

[16] D.M. Weber, P.W.M. Brighton, Similarity solutions for the spreading of liquid pools, UKAEA Report SRD R371, 1986.

[17] D.M. Weber, P.W.M. Brighton, An integral model for spreading of vaporizing pools, derived from shallow-layer equations, UKAEA Report SRD R390, 1987.

[18] T.K. Fannelop, G.D. Waldman, Dynamics of oil slick, Am. Inst. Aeronaut. Astronaut. J. 10 (1972) 506–510.

[19] D.P. Hoult, Oil spreading on the sea, Annu. Rev. Fluid Mech. 4 (1972) 341–368.

[20] H.R. Chang, R.C. Reid, Spreading-boiling model for instantaneous spills of liquefied petroleum gas (LPG) on water, J. Hazard. Mater. 7 (1982) 19–35.

[21] J. Cook, J.L. Woodward, A New Integrated Model for Pool Spreading, Evaporation and Solution on Land and Water. Health, Safety and Loss Prevention in the Oil, Chemical and Process Industry, Butterworth, Oxford, 1993, pp. 359–370.

[22] T.A. Cavanaugh, J.H. Siegell, K.W. Steinberg, Simulation of vapor emissions from the liquid spills, J. Hazard. Mater. 38 (1994) 41–63.

[23] P.L. Yue, M.E. Weber, Minimum film boiling flux for binary mixtures, Trans. Instit. Chem. Eng. 52 (1974) 217–221.

[24] V.V. Klimenko, Film boiling on a horizontal plate—new correlation, Int. J. Heat Mass Transfer 24 (1981) 69–79.

[25] G. Opschoor, Investigation into the evaporation of liquefied gases spilled on water, TNO Report 80-05624, Bureau IndustrieleVeiligheid TNO, Rijswijk, The Netherlands, 1980.

[26] P.K. Raj, A.S Kalelkar, Assessment Models in Support of the Hazard Assessment Book (CG-446-3), US Coast Guard, Washington DC, 1974, see also P.K. Raj, Report No. AD776617, US Coast Guard, Springfield, Virginia, 1974.

[27] H.S. Carslaw, J.C. Jaeger, Conduction of Heat in Solids, 2nd ed., Oxford University Press, Oxford, 1959, pp. 70–73.

[28] W.D. Murray, F. Landis, Numerical and machine solutions of transient heat conduction problems involving melting or freezing, J. Heat Transfer 81 (1959) 106–120.
[29] E. Guerra, Modeling the vaporization rate of LNG, MSc thesis, Imperial College London, London 2001.
[30] R.E. Henry, A correlation for the minimum film boiling temperature, AIChE Sym. Series 70 (1974) 987–989.
[31] K.J. Baumeister, F.F. Simon, Leidenfrost temperature—its correlation for liquid metals, cryogens, hydrocarbons and water, Trans. ASME, J. Heat Transfer (1973) 166–173.